

INVESTIGATION EFFECTS OF BACKWARD AND FORWARD BLADE SKEW MODES APPLIED TO AXIAL FLOW TURBO MACHINERY

ADEL.M.AL. JAMOM¹

Institute of Science and Technology-Zawiya-Libya

Abstract - Since the three-dimensional (3D) Computational fluid dynamic (CFD) flow field investigation techniques, as well as advanced flow measurement tools, give potential to predict effects related to blade skew to consider them in blade design.

Through the use of CFD tools and the analysis of experimental data that has been published in the literature, the effects of skew applied to the rotor of axial flow turbo engines were examined in this work. Low-aspect-ratio rotors with forward and backward skew have been investigated, and their performance has been compared to that of un-skew datum rotors at various flow rates, span wise positions, and overall efficiency. In this work, the blade sections are swept forward and backward with 3.5 degree and 2.082 degree for dihedral as comparison with data in research and development (R&D) in the field of axial flow turbo machinery (such as fan, compressor, pump) at nowadays. It is focuses on isolated rotors of fluid transporting machines to improve the rotor performance characteristics via the beneficial modification on blade aerodynamics, by means of appropriate modification of blade geometry. Nowadays, the enhanced computational resources allow the designer to realize blade design concepts being more sophisticated and complicated than the "classic" designs, e.g. incorporating blade sweep with aid of Computational Fluid Dynamics (CFD) simulations. Three-dimensional (3D) CFD flow field investigation techniques, as well as advanced flow measurement tools, give potential to predict effects related to blade sweep and skew to consider them in blade design. It was noted that FSK provides a greater efficiency up to 75% of the blade span at the design point, demonstrating the advantages of FSK rotors over other rotors.

Near the tip and at smaller radii, the forward-skewed blade increased and decreased inlet axial velocities, respectively. Due to the small skew angles, the three rotors nearly have similar outlet axial velocities performance. The axial velocity also increases along the dominant part of the span.

At the design flow rate, the forward skew considerably reduces the radically outward flow along the span and mostly near the tip.

Key Words: axial flow rotors, backward skew, forward skew, controlled vortex design.

1.INTRODUCTION

Axial flow fans are frequently used in engineering and industrial settings. Many researches were carried out for improving the efficiencies by modifying certain geometric features, such as imparting blade sweep and/or skew for development of aerodynamic optimum shape of turbo machinery balding. Computational fluid dynamic (CFD) and numerical simulation have been widely applied in optimization design of fan blades. Up-to-date CFD techniques are available for the reliable prediction of 3D turbo machinery flow. Since measurements are expensive, time-consuming and strongly limited from the viewpoint of airfoil variations under investigation, it is beneficial to use CFD tool, which simulates the flow past the cascade of airfoils in a realistic manner. By doing so, it is possible to assess the effects of airfoil shape adjustments on the flow field quickly and more effectively determine the best practices for aerodynamic optimization. It appears to be beneficial to supplement these techniques with analytical models for exploring the underlying physics of 3D flow effects. By using computational fluid dynamic (CFD) techniques and processing experimental data that has been published in the literature, the study aims to evaluate the impact of skew applied to the rotor of axial flow turbo engines. At various span-wise positions, low-aspect-ratio rotors with forward and backward skew have been explored and contrasted with unskew datum rotors. Comparative studies have been carried out on these three rotors at the design flow rates by means of developing structured fully hexahedral mesh of the entire computational domain. The efficiency as well as the losses will be detected on all type of rotors along the span. In order to obtain information on the inter blade flow details, a CFD technique has been developed, using the finite-volume code FLUENT [1]. Using some data obtained for circumferential forward-skewed (FSK) of work of [2], the CFD tool was enabling us to use fixed blade chord along the span for BSK, FSK and USK rotors.

2-STRUCTURED GRIDS USED FOR USK, FSK AND BSK ROTORS

The flow fields in BSK, FSK and USK rotors were simulated by means of the same CFD codes. The computation domain for BSK, FSK and USK rotors has been regarded one blade pitch only. Typical computational domains for USK rotor are presented in Figure1.

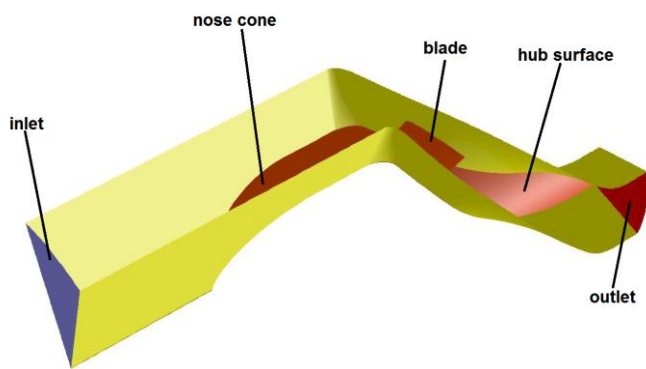


Fig-1: Computational domain for USK rotor

The inlet face is a sector of the circular duct with 30 deg central angle. Downstream of the inlet face, sectors of the steady inlet cone and the rotating hub with one blade in the middle of the domain are included for both types of blading. At the inlet face, a swirl-free uniform axial inlet condition corresponding to the actual flow rate has been prescribed. The casing diameter was used as the hydraulic diameter to calculate the turbulence length scale, with the inlet turbulence intensity set to 1 percent. The rotor's meshing features are shown in Figure 2. At the outlet boundary (outflow condition in FLUENT), all flow variables have been subjected to a zero diffusion flux condition [1].

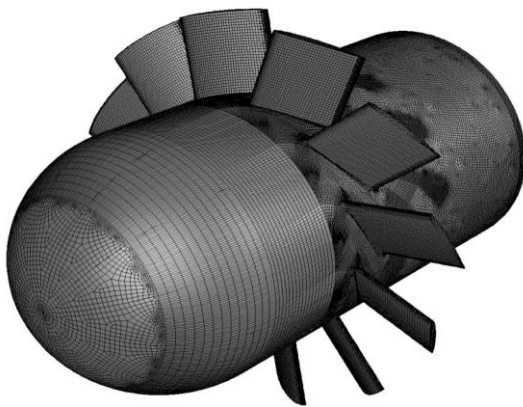


Fig-2: Meshing details for USK rotor

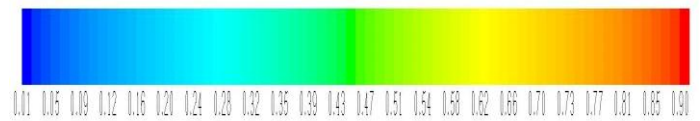
The equiangular skewness of a cell is defined as the maximum value of the ratio of actual and possibly highest deviation from the optimum angle, considering each vertex [1]. Decreasing of equiangular skewness was achieved in structured grid. The grid design ensures that 99 % of the cells have equiangular skewness less than 0.6, and the maximum skewness value is 0.71. As the figure suggests, the highest skewness values appear near the LE and TE. Over the dominant part of the SS and PS, the skewness is less than 0.35. Figure 3(b) shows the skewness values of the near-blade cells for USK along the axial chord, with zero axial position at the LE at mid span.

Table -1: Skewness Value

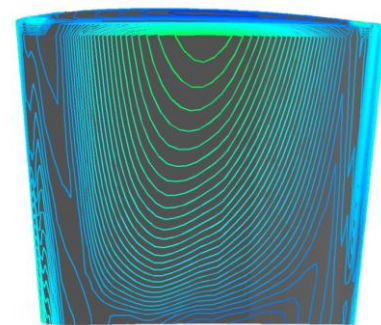
From above, by evaluating the results of figure (3.a) the

Value of Skewness	0-0.25	0.25-0.50	0.50-0.80	0.80-0.95	0.95-0.99	0.99-1.00
Cell Quality	excellent	good	acceptable	poor	sliver	degenerate

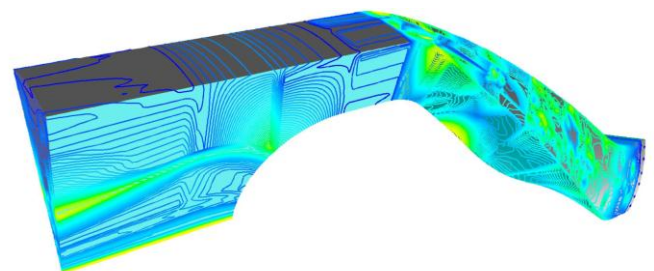
value of the skewness is about 0.29 which is good according to table1.



(a)



(b) Blade



(c) Domain

Fig-3: Distribution of cell equiangular skew

3. Program structure

FLUENT package includes the following products:

- GAMBIT (re-processor): for geometry modeling and mesh generation.
- FLUENT (post-processor)[1].

4. Boundary Conditions

1-The inlet boundary condition is set as a velocity inlet where the velocity value is 9.2 [m/s] design flow rate . The flow direction is parallel to the rotational axis, which means the direction of x.

2- The blade, hub and outer case have been defined as wall, which does not let through the flow and create the boundary layers around them.

3- Outflow is used for the condition of outlet boundary.

4- the remaining part of the domain is set as default interior and the fluid boundary condition is applied for this domain where the air density is constant with the value of $\rho_{air}=1.225$ [kg /m³]

5- All the side surfaces of the domain are defined as rotational periodic.

5. COMPARATIVE CFD STUDIES ON BSK, FSK AND USK AT ROTORS AT THE DESIGN FLOW RATE

The axial fan is used as the research target, and the computational fluid dynamics method is used to simulate the three-dimensional flow of the axial fan. First, the modeling of an axial fan is introduced. The inlet (1) and outlet (2) planes have the axial position of -20.0 and 113.0 percent mid-span axial chord, respectively, where the zero axial position indicates the LE at mid-span as shown in Figure 4.

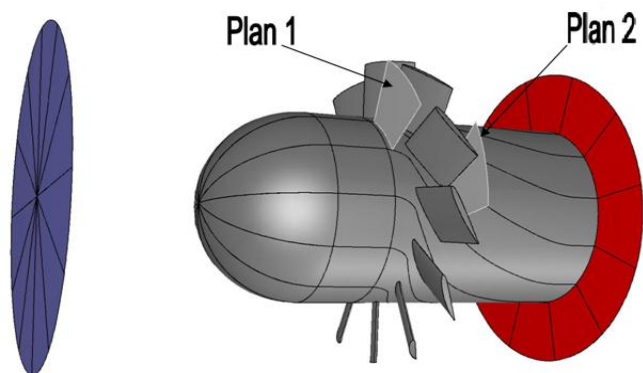


Fig-4: USK Rotor with indication of planes 1 and 2

The relationship between the skew and un-skew parameters blades and the total pressure and the efficiency of the axial fan were investigated. After that, the qualitative comparison between BSK, FSK and USK rotors at the design flow rate is developed to solve the complex multi objective optimization problem where the total pressure and the efficiency of the axial fan are the optimization objectives. Finally, some conclusions are presented. The characteristics and efficiency curves, the computational mesh and boundary conditions of the axial fan are presented in the following sections.

5. RESULTS AND DISCUSSIONS

5.1. Inlet axial velocity coefficient

Compare with other contributions, the inlet flow field has been investigated for USK, FSK and BSK. The near-tip part of the forward-skewed blade protrudes into the upstream relative flow field, and carries out work in advance compared to the blade sections at lower radii. This is suggested also by the generally increased axial velocity near the FSK LE as explained by Figure 5. This results in locally increased inlet axial velocity near the tip, results in the reduction of inlet axial velocity at lower radii of FSK. The same result was suggested by [3]. The inlet axial velocity profile has been found practically identical for the three rotors as shown in Figure 6. It seen that the near-tip part of the forward-skewed blade carries out work in advance compared to the blade sections at lower radii. This increases inlet axial velocity near the tip. Increase of inlet axial velocity near the tip results in the reduction of inlet axial velocity at lower radii of FSK. The applied blade FSK has an influence on the rotor inlet flow field: the inlet axial velocity for FSK is increased at the mid span especially at 70% span and is reduced at lower radii, as was observed for FSK rotors also in [4] this effect can be confirmed as a sort of sweep rather than dihedral.

TABEL - 2: Inlet flow readings

sigma	INLET FLOW		
	@-FSK	@-USK	@-BSK
0			
0.045455	0.275799	0.277612	0.277357
0.090909	0.30489	0.305663	0.306251
0.136364	0.31301	0.313279	0.314285
0.181818	0.318034	0.319277	0.319216
0.227273	0.323167	0.323294	0.324224
0.272727	0.326746	0.326904	0.327675
0.318182	0.330493	0.330157	0.33125
0.363636	0.333153	0.332637	0.333757
0.409091	0.335903	0.335024	0.336306
0.454545	0.337813	0.337055	0.338049
0.5	0.339675	0.338569	0.339713
0.545455	0.340866	0.339883	0.340745
0.590909	0.341847	0.340742	0.34153
0.636364	0.342315	0.341202	0.341837
0.681818	0.34241	0.341318	0.34176
0.727273	0.342166	0.341022	0.341382
0.772727	0.341395	0.34035	0.340458
0.818182	0.340445	0.338942	0.339394
0.863636	0.33844	0.336886	0.337261
0.909091	0.335014	0.333075	0.333736
0.954545	0.304674	0.310086	0.303106

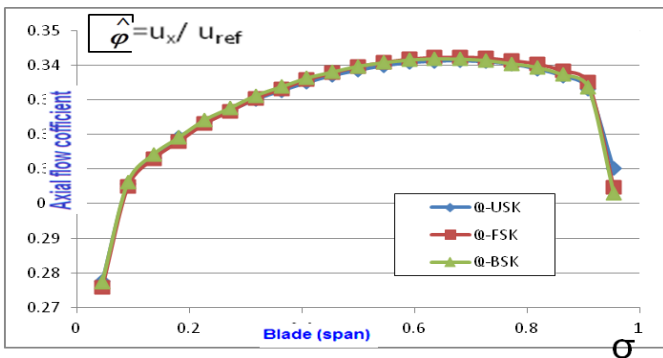


Fig-5: Span wise distributions of pitch-averaged of inlet axial velocity coefficient at the design flow rate.

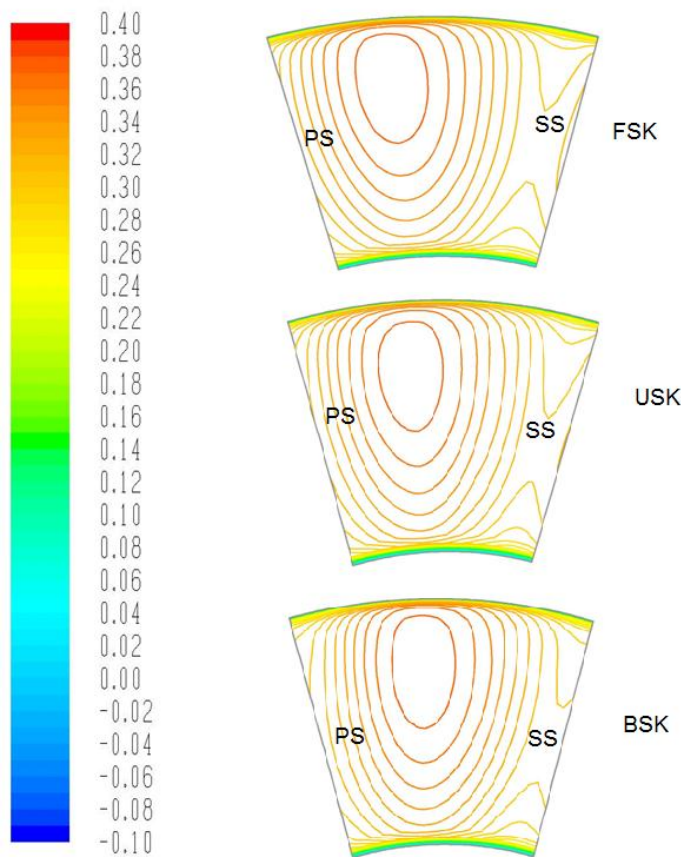


Fig-6: Distributions of pitch-averaged of inlet axial velocity coefficient.

5.2.Outlet axial velocity coefficient

Figures 7 and 8 indicate that, the three rotors having nearly similar axial velocities performance, this may be possibly due to the small skew angle. Due to the reduced size of the stagnating zone near the tip, the near-casing layer of reduced total pressure rise and axial velocity is slightly thinner in the case of skew [5]. The axial velocity also increases along the dominant part of the span as indicated by Figure 6. that, the aerodynamic optimization design of forward-skewed blade of low-pressure axial flow fan indicate that the impeller with forward-skewed blades would cause a span wise redistribution of flow rate and pressure toward the blade mid-span, as well as reduce tip loading as shown by [6]. Furthermore, the locus of maximum axial velocity is shifted toward higher radii. This results in increased pitch wise area averaged axial velocity near the tip of FSK and BSK as shown in Figures 5.

TABEL - 3: Outlet flow readings

sigma	Outlet Flow		
	@-FSK	@-USK	@-BSK
0			
0.045455	0.23263	0.229338	0.235929
0.090909	0.272287	0.268923	0.273362
0.136364	0.289379	0.287064	0.290108
0.181818	0.299636	0.297879	0.299996
0.227273	0.310745	0.309278	0.31071
0.272727	0.320734	0.319477	0.320022
0.318182	0.3318	0.330611	0.33058
0.363636	0.341857	0.340806	0.339882
0.409091	0.35278	0.351673	0.350194
0.454545	0.362799	0.361666	0.359263
0.5	0.373713	0.372348	0.369325
0.545455	0.383766	0.382318	0.378232
0.590909	0.395135	0.393409	0.388456
0.636364	0.405894	0.403947	0.397793
0.681818	0.418851	0.415954	0.409248
0.727273	0.431101	0.426558	0.419892
0.772727	0.444234	0.437112	0.431608
0.818182	0.441205	0.437099	0.431412
0.863636	0.353942	0.368714	0.362796
0.909091	0.189944	0.204703	0.21357
0.954545	-0.00571	-0.00077	0.02304

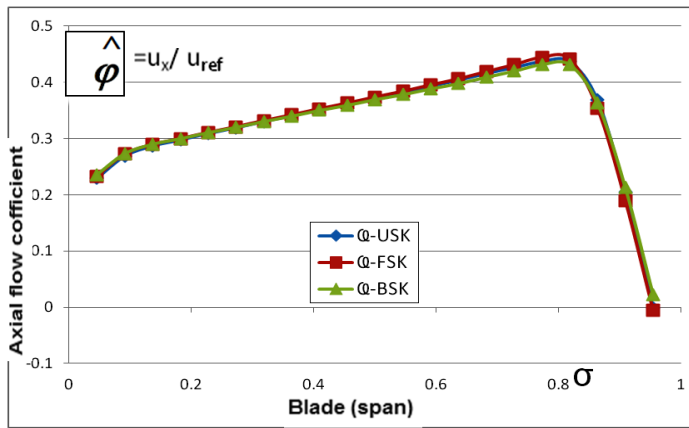


Fig- 7: Span wise distributions of pitch-averaged of the outlet axial velocity coefficient at the design flow rate .

5.3.Total efficiency

The distributions of the local and pitch-averaged total efficiencies are presented. Figures 9 and 10 indicate that FSK and BSK rotors operate at higher efficiency than USK. The Local total efficiency has been defined as the ratio between the local total pressure rise and the ideal local total pressure rise. The latter was computed using the Euler equation of turbo machines as a product of density, blade circumferential velocity at the given radius, and local absolute tangential fluid velocity at the outlet. The higher efficiency of FSK occurs up to 75% blade span which demonstrates the benefits of FSK rotor. In the near-casing zone all rotors demonstrate the same results.

TABEL - 4: Total efficiency readings

sigma	Total efficiency		
	η-FSK	η-USK	η-BSK
0			
0.045455	0.60532	0.571362	0.577276
0.090909	0.735076	0.700468	0.714509
0.136364	0.781872	0.749622	0.764419
0.181818	0.796102	0.76681	0.780265
0.227273	0.806211	0.780468	0.792037
0.272727	0.813517	0.790853	0.800353
0.318182	0.82058	0.801125	0.808655
0.363636	0.82591	0.809075	0.814663
0.409091	0.831033	0.8167	0.820517
0.454545	0.834805	0.822322	0.824622
0.5	0.838337	0.827755	0.828579
0.545455	0.840955	0.831849	0.831273
0.590909	0.843652	0.836266	0.834129
0.636364	0.845955	0.839624	0.836411
0.681818	0.848055	0.842088	0.838781
0.727273	0.846295	0.840412	0.837992
0.772727	0.816425	0.82442	0.813843
0.818182	0.70612	0.758822	0.719623
0.863636	0.492751	0.53674	0.508108
0.909091	0.346111	0.347732	0.346223
0.954545	0.235359	0.228518	0.241963

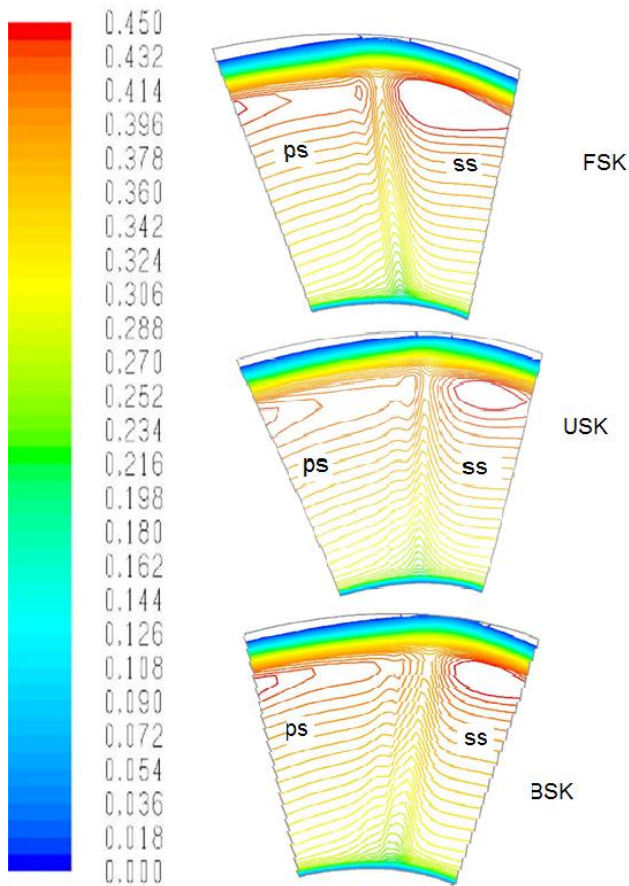


Fig- 8: distributions of the local axial velocity coefficient at the outlet plan.

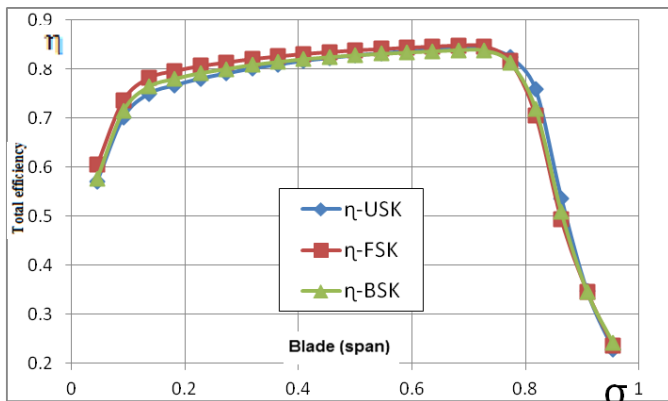


Fig- 9: span wise distribution of local total efficiency at design flow rate.

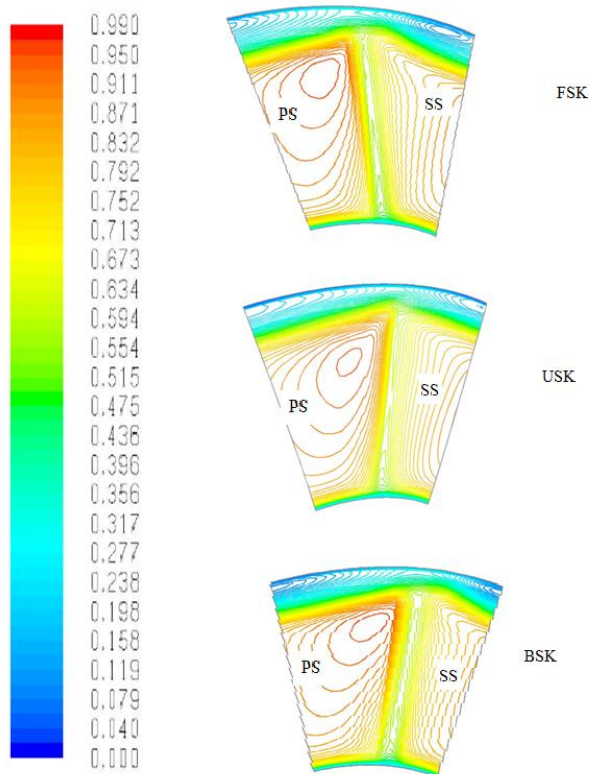


Fig- 10: Span wise distributions of local total efficiency at the design flow rate.

6. Conclusions

An axial fan rotor of Controlled Vortex Design, having forward and backward skew has been subjected to CFD investigation. It has been compared to an un-skewed datum rotor at its design flow rate. The CFD studies were supported by global performance measurements of literatures. The results illustrated and summarized as follows:

1. The circumferentially forward-skewed blade tip carries out work on the incoming fluid in advance compared with the blade sections at lower radii. This results in increased and decreased inlet axial velocities near the tip and at lower radii, respectively.

2- The three rotors having nearly similar outlet axial velocities performance, this is may be possibly due to the small skew angles. The axial velocity also increases along the dominant part of the span.

3- At the design flow rate, in the near-casing zone all rotors demonstrate the about the same results of efficiency. The higher efficiency of FSK occurs up to 75% blade span which demonstrates the benefits of FSK rotor.

4- Due to forward skew, the isobars are inclined “more forward” for FSK than for USK and BSK. The mechanism by which forward skew attenuates the SS radial outward flow.

REFERENCES

- [1] FLUENT (FLUENT 6.3.26, 2006) , Fluent Inc., Lebanon, NH, USA.
- [2] Vad , J., Kwedikha, A. R. A., Kristóf, G., Lohász, M. M., Rábai, G., Rácz, N. and Watanabe, K. , 2005, “Effects of blade skew in an axial flow rotor of controlled vortex design.” 6th European Conference on Turbomachinery Fluid Dynamics and Thermodynamics, Lille Proceedings pp. 46-55.
- [3] JvAd *,ARAKwedikha, Cs Horváth, M Balczó, M M Lohász, andT Réger (2009). Aerodynamic effects of forward blade skew in axial flow rotors of controlled vortex design - Proc. IMechE Vol. 221 Part A: J. Power and Energy Ali R. A. Kwedikha, Aerodynamic effects of blade sweep and skew applied to rotors of axial flow turbomachinery -Budapest.
- [4] Meixner, H. U. (1995), Vergleichende LDA-Messungen an ungesicherten und gesicherten Axialventilatoren. Dissertation Universität Karlsruhe, VDI-Verlag, Reih7: Strömungstechnik, No. 266, Düsseldorf.
- [5] Vad, J., Kwedikha, A. R. A., Horva'th, Cs., Balczo', M., Loha'sz, M. M., and Re'gert, T.(2007). “Aerodynamic effects of forward blade skew in axial flow rotors of controlled vortex design”. Proc. IMechE, Part A: J. Power and Energy, 2007, 221, 1011-1023.
- [6] Li Yang, OuyangHua, and Du Zhao-Hu . (2007). Optimization Design and Experimental Study of Low-Pressure Axial Fan with Forward-Skewed Blades – Hindawi Publishing Corporation International Journal of Rotating Machinery Volume 2007, Article ID 85275, 10 pages - doi:10.1155/85275.